IUST
Iran University of Science and Technology

Iranian Journal of Electrical and Electronic Engineering

Journal Homepage: ijeee.iust.ac.ir

Research Paper

Optimal Operation of Doubly-fed Induction Generator used in a Grid-Connected Wind Power System

H. Gasmi*(C.A.), M. Sofiane**, H. Benbouhenni***, and N. Bizon****

Abstract: In this paper, a wind power system based on a doubly-fed induction generator (DFIG) is modeled and simulated. To guarantee high-performance control of the powers injected into the grid by the wind turbine, five intelligent super-twisting sliding mode controllers (STSMC) are used to eliminate the active power and current ripples of the DFIG. The STSMC controller is a high-order sliding mode controller which offers high robustness compared to the traditional sliding mode controller. In addition, it reduces the phenomenon of chattering due to the discontinuous component of the SMC technique. However, the simplicity, ease of execution, durability, and ease of adjusting response are among the most important features of this control compared to some other types. To increase the robustness and improve the response of STSMC, particle swarm optimization method is used for this purpose, where this algorithm is used for parameter calculation. The simulation results obtained using MATLAB software confirm the characteristics of the designed strategy in reducing chattering and ensuring good power control of the DFIG-based wind power.

Keywords: Sliding Mode Control, Doubly-fed Induction Generator, Super-twisting Sliding Mode Controller, Particle Swarm Optimization, Wind Turbine.

1 Introduction

WIND power (WP) is currently one of the most exploited renewable sources in the world and its market share continues to grow steadily. Turbines called wind turbines are used to exploit WP, as there are two types of turbines.

Iranian Journal of Electrical and Electronic Engineering, 2023.
Paper first received 17 Feb 2022, revised 23 Mar 2023, and accepted 28 Mar 2023.
*Laboratoire de Contrôle Avancé (LABCAV), Department of Electronics and Telecommunications, Université 8 Mai 1945 Guelma, Guelma, Algeria.
E-mail: gasmi.hamza@univ-guelma.dz.
**Department of Electrical Engineering and Automation, Université 8 Mai 1945 Guelma, Guelma, Algeria.
E-mail: mendaci.sofiane@univ-gulma.dz.
***Faculty of Engineering and Architecture, Department of Electrical & Electronics Engineering, Nisantasi University, 34481742 Istanbul, Turkey.
E-mail: habib.benbouenni@nisantasi.edu.tr.
****Faculty of Electronics, Communication and Computers, University of Pitesti, 110040 Pitesti, Romania.
****Doctoral School, Polytechnic University of Bucharest, 313 Splaiul Independentei, 060042 Bucharest, Romania.
****ICSI Energy, National Research and Development Institute for Cryogenic and Isotopic Technologies, 240050 Ramnicu Valcea, Romania.
E-mail: gasmi.hamza@univ-guelma.dz.
Corresponding Author: H. Gasmi.
https://doi.org/10.22068/IJEEE.19.2.2431.

The first type is horizontal wind turbines and the second type is vertical wind turbines. The use of wind energy to generate electric power greatly helps to protect the environment, reduce the cost of electricity, and reduce the focus on the use of traditional energy sources. Due to its remarkable advantages, a doubly-fed induction generator (DFIG) is widely used in WP systems, particularly in wind farms. It has exceptional advantages, such as the ability to regulate reactive and active powers, variable speed operation, low cost, easy to control, high durability, reduced efforts on mechanical parts, and the use of a low-rated-power converter in the rotor (30% of rated power) [1-2].

To regulate the active power of the DFIG-based WP systems, several control strategies were used, to ameliorate the quality of the produced current and reduce the THD (Total Harmonic Distortion) value of voltage/current. These control strategies used differ in principle and the use of the type of controller, as some control strategies use proportional-integral (PI) controllers such as direct and indirect field-oriented control (FOC) techniques [3]. Some control strategies are based in

principle on the use of switching tables and hysteresis comparators to regulate the basic ingredients such as the DTC (Direct Torque Control) method [4], the DPC (Direct Power Control) technique [5]. There are other nonlinear control strategies used to control the DFIG-based WP system such as synergetic control [6], sliding mode control (SMC) [7], backstepping control [8], and terminal synergetic control [9]. These nonlinear control strategies are characterized by their robustness and provide very satisfactory results compared to the classical techniques such as DTC and DPC techniques.

Traditional control techniques based on the traditional PI controller provide adequate performance in a variety of industrial applications, but they have many drawbacks, such as the difficulty of controlling non-linear systems and the sensitivity to fluctuations of the system parameters and measurement errors. Several new nonlinear control techniques have been developed over the years to replace traditional PI controllers to ameliorate robustness and efficiency.

Conventionally, the SMC method is one of the nonlinear strategies widely used in different fields because of its natural ability to effectively control uncertain and/or nonlinear systems [10-11]. In [12], SMC based on a neural algorithm was designed to command the rotor side converter (RSC) of the DFIG. The designed neural SMC technique is a simple controller and more robust than the classical SMC strategy. In the neural SMC technique, the function Sign of the SMC strategy was replaced by a neural network (NN). Another intelligent SMC technique was proposed in [13] to control the DFIG. This suggested control strategy is to use the fuzzy SMC controller, this is to overcome the problems and disadvantages of the traditional control strategy. The simulation results showed the characteristics of the designed strategy (fuzzy SMC) in minimizing chattering problems compared to the traditional SMC. The chattering problem is among the most common problems in SMC and this is due to the use of the function Sign.

Because of the chattering problem, that characterizes the classical SMC technique, various ideas have emerged to minimize the chattering effect without degrading the well-known robustness of the SMC. Integral-SMC [14], SMC with a novel exponential reaching law (NERL) [15], SMC combined with intelligent strategies [16-18], and high-order SMC strategy [19-23] are one of the proposed control strategies in the literature to reduce the chattering phenomenon caused by the high-speed switching control law. In [24], a new nonlinear technique was designed to ameliorate the quality of the active power and current of the DFIG-based dual-rotor wind power (DRWP). This proposed nonlinear strategy is based on a third-order SMC (TOSMC) strategy. However, the TOSMC is a simple controller and more robust than the traditional SMC strategy. Another nonlinear technique was designed based on the TOSMC controller and NN technique to reduce the current and active power undulations of the DFIG-DRWP system [25]. The proposed neural TOSMC controller is a robust technique compared to the classical SMC controller and TOSMC strategies. All the nonlinear control strategies mentioned in this work, which were not mentioned, have advantages and disadvantages that distinguish them from each other. However, super-twisting SMC (STSMC) controller remains among the most simple and easy to implement nonlinear methods compared to other strategies such as SMC and SOSMC techniques, where this method can be applied easily and does not require mathematical calculations or the mathematical form of the studied system, similar to the classical method (SMC strategy) [26]. Several scientific works used this method, and all of them agreed that this method is a simple controller and gives better results compared to both SMC and SOSMC techniques. In [27], the author proposed to use of the STSMC controller to ameliorate the performances of the five-phase induction machine. Experimental results showed how easy it is to apply this method and how effective it is compared to the traditional control. By observing the results, the use of the STSMC method led to a decrease in the value of THD of current and a reduction in the torque ripples of the machine compared to the classical strategy. Despite the experimental results obtained in [27], these still give undesirable results. This method does not completely remove the chattering problem, it reduces it. Several works dealt with the disadvantages of the STSMC technique and an attempt to ameliorate the characteristic and effectiveness of the traditional STSMC strategy. In [28], the author proposed a new STSMC algorithm to regulate the reactive and active powers of the DFIG-based WP system. The proposed STSMC controller is based on a neural algorithm to minimize the torque ripple and THD value of voltage. STSMC controller and fuzzy technique were combined to regulate the current and active

power of the DFIG [29]. Another intelligent STSMC algorithm was proposed in [30], to regulate the flux and torque of the DFIG [30]. This proposed STSMC algorithm is based on the neuro-fuzzy controller. However, the STSMC technique based on a neuro-fuzzy algorithm is more robust compared to the classical STSMC strategy.

In this study, an intelligent STSMC controller is used to ensure the MPPT (maximum power point tracking) technique and to regulate the current and active power exchanged between the DFIG and the grid. However, due to the large number of parameters to be tuned of the five STSMC controllers used in the designed structure, impossible to adjust manually, the PSO (particle swarm optimization) algorithm is used to find the best parameters. Simulation results show that the control scheme based on the proposed PSO-STSMC algorithms ameliorates the characteristic of the DFIG-based wind power system over a wide range of wind speed variations compared to the traditional SMC technique.

This paper puts forward a novel indirect FOC strategy, shows the results of the relevant simulation of the DFIG-based WP system, and compares the designed nonlinear strategy with the traditional SMC technique. The objective of this work is to apply the proposed PSO-STSMC algorithm to ameliorate the characteristics of the indirect FOC strategy of the DFIG. The simulation results validate that the indirect FOC technique with the proposed PSO-STSMC algorithms has very robust behavior and it works with minimum active and reactive power undulations, overshoot, and steady-state error. So, this proposal represents a new robust and ripple-free indirect FOC strategy for the DFIG drive control.

To understand the work in this paper, we make a simple diagram called a diagram of the design. A diagram of the design, testing and validation stages of the indirect FOC technique with the proposed PSO-STSMC algorithm using MPPT-PSO-STSMC technique is shown in Fig. 1.

The main contributions of the work are listed below:

- A new MPPT technique is designed for the wind turbine.
- The new STSMC controller is proposed based on the PSO algorithm to ameliorate the effects of the DFIG.
- The proposed nonlinear indirect FOC technique is a robust control scheme and therefore easier to implement compared to other existing strategies. Also, the designed nonlinear indirect FOC technique minimizes the current, torque, voltage, reactive power, rotor flux, and active power ripples and reduces the THD value of the voltage of DFIG-based WP system compared to other reference techniques designed in the literature.
- Reduced power ripple, overshoot, and steady-state error (SSE) compared to SMC control.

This paper is organized as follows. Section 2 presentation of modeling of the wind turbine. Section 3 explains the SMC control scheme for the DFIG. The designed PSO-STSMC controller is presented in Section 4. Section 5 explains the proposed indirect FOC strategy based on the proposed PSO-STSMC controller for the DFIG-based wind turbine. Numerical simulation studies are presented in Section 6. The conclusion is given in Section 7.

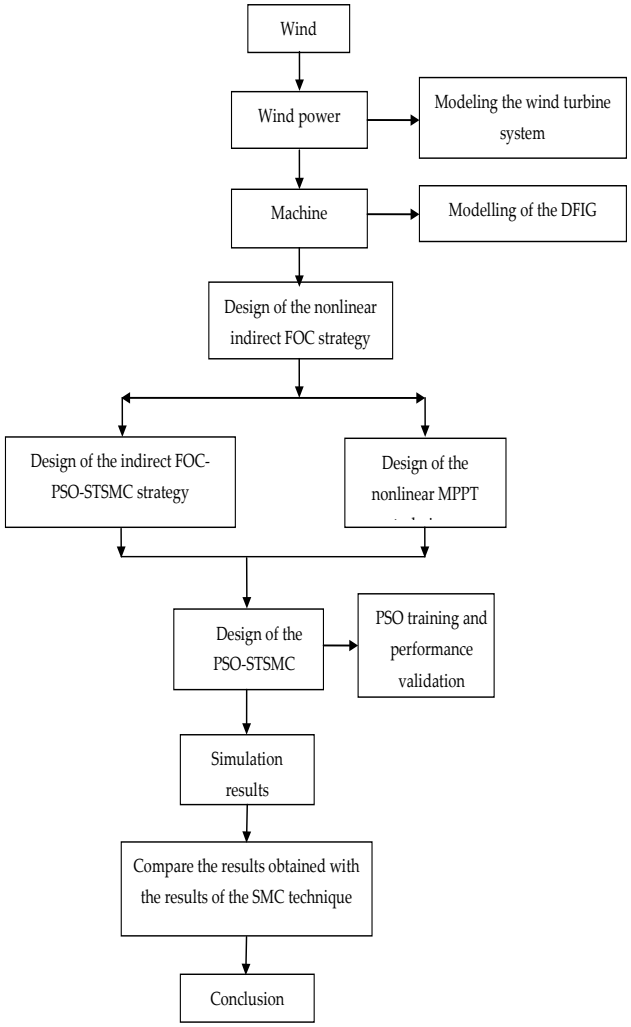

Fig. 1 Diagram for designed technique.

2 Modelling of WP System

Figure 2 shows the basic configuration of a DFIG-based WP system. It consists of turbine, a

gearbox, a back-to-back converter, and a DFIG connected to the grid. The DFIG stator supplies energy to the grid, while the rotor can absorb or supply it, depending on the generator speed.

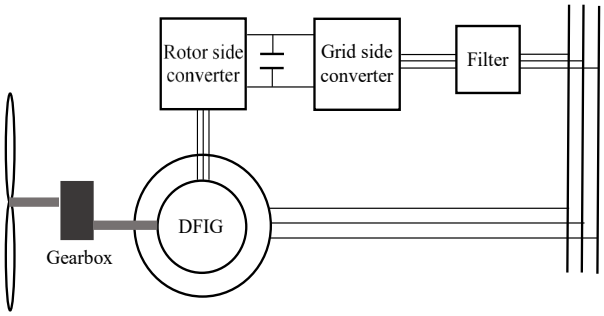

Fig. 2 Structure of the studied DFIG wind turbine.

2.1 Wind turbine model

The power received from the wind by the turbine is approximated by the following equation [31]:

$$P_v = 0.5\rho S_w v^3 \tag{1}$$

where, R is the blade length, C_p is the power coefficient, V is the wind speed, and ρ is the air density, [2]. It is modelled by:

$$C_p(\lambda,\beta) = \frac{46}{100}\left(\frac{151}{\lambda_i} - \frac{58}{100}\beta - \frac{2}{1000}\beta^{2.14} - 13.2\right)e^{\frac{-18.4}{\lambda_i}} \tag{2}$$

$$\lambda_i = \frac{1}{\lambda + 0.02\beta} - \frac{0.003}{\beta^3 + 1} \tag{3}$$

$$\lambda = \frac{R\Omega_t}{V} \tag{4}$$

The aerodynamic torque is expressed as following:

$$T_{aer} = \frac{1}{2\Omega_t}\rho\pi R^2 C_p(\lambda,\beta)\mathrm{V}^3 \tag{5}$$

The role of the gearbox is to adapt the low speed Ω_t of the turbine rotor to the high speed Ω_m of the generator:

$$\begin{cases} T_m = \dfrac{T_{aer}}{G} \\ \Omega_m = G\Omega_t \end{cases} \tag{6}$$

where, T_m is the mechanical torque at the generator side.

The dynamic model of the rotating parts of the wind power is conventionally given by the following equation:

$$J_{tot}\frac{d\Omega_m}{dt} = T_g - T_{em} - f\Omega_m \tag{7}$$

where, f is the total friction, J_{tot} is the moment of inertia of the rotating parts, and T_{em} is the torque produced by DFIG.

2.2 DFIG model

The DFIG electrical equations can be represented in d-q synchronous reference frame by [24, 32]:

$$\begin{cases} V_{ds} = R_s I_{ds} + \dfrac{d\varphi_{ds}}{dt} - w_s\varphi_{qs} \\ V_{qs} = R_s I_{qs} + \dfrac{d\varphi_{qs}}{dt} + w_s\varphi_{ds} \\ V_{dr} = R_r I_{dr} + \dfrac{d\varphi_{dr}}{dt} - (w_s - w_r)\varphi_{qr} \\ V_{qr} = R_r I_{qr} + \dfrac{d\varphi_{qr}}{dt} + (w_s - w_r)\varphi_{dr} \end{cases} \tag{8}$$

Further, the stator and rotor flux expression are as follows:

$$\begin{cases} \varphi_{ds} = MI_{dr} + L_s I_{ds} \\ \varphi_{qs} = MI_{qr} + L_s I_{qs} \\ \varphi_{dr} = MI_{ds} + L_r I_{dr} \\ \varphi_{qr} = MI_{qs} + L_r I_{qr} \end{cases} \tag{9}$$

where, V_{ds}, V_{qs}, V_{dr}, and V_{qr} are the d-q axes voltage components of the stator and rotor, respectively. I_{ds}, I_{qs}, I_{dr}, and I_{qr} are the stator and rotor d-q axes currents, respectively. φ_{ds}, φ_{qs}, φ_{dr}, φ_{qr}, are the stator and rotor flux components, respectively.

Equation (10) expresses the active and reactive power, where these two capacities are calculated using the measured voltage and current. Therefore, high-precision measuring devices must be used to reduce measurement error.

$$\begin{cases} P_s = V_{qs} I_{qs} + V_{ds} I_{ds} \\ Q_s = -V_{ds} I_{qs} + V_{qs} I_{ds} \end{cases} \tag{10}$$

If the stator resistance R_s is neglected and the φ_s is assumed to be constant and oriented along the d-axis, the two stator voltage equations become as follows [14, 22]:

$$\begin{cases} V_{ds} = 0 \\ V_{qs} = V_s = w_s\varphi_s \end{cases} \tag{11}$$

$$\begin{cases} \varphi_{qs} = \varphi_s = cte \\ \varphi_{ds} = 0 \end{cases} \tag{12}$$

The reactive and active power equations can be written, as a function of the current rotor d-q components, as follows:

$$\begin{cases} P_s = V_{sq} I_{sq} \\ Q_s = V_{sq} I_{sd} \end{cases} \tag{13}$$

The rotor voltage equations can be simplified as:

$$\begin{cases} V_{dr} = R_r I_{dr} + \sigma L_r \dfrac{dI_{dr}}{dt} - \sigma L_r w_r I_{qr} \\ V_{qr} = R_r I_{qr} + \sigma L_r \dfrac{dI_{qr}}{dt} + \sigma L_r w_r I_{dr} + w_r \dfrac{M}{L_s}\varphi_s \end{cases} \quad (14)$$

$$\sigma = 1 - \frac{M^2}{L_r L_s} \quad (15)$$

Then, the quadrature and direct rotor currents can be expressed as:

$$\begin{cases} \dot{I}_{dr} = \dfrac{1}{\sigma}(V_{dr} - R_r I_{dr} + s w_S \sigma I_{qr}) \\ \dot{I}_{qr} = \dfrac{1}{\sigma}(V_{qr} - R_r I_{qr} - s w_S \sigma L_{dr} - s w_S \dfrac{M}{L_S}\varphi_S) \end{cases} \quad (16)$$

There are several control strategies used to control generators, and the most famous of these methods are non-linear methods that depend on the use of the SMC strategy. This technique is more robust than the DTC strategy, FOC strategy, and DPC strategy. The DFIG control is dealt with using the SMC, and this depends on the MPPT technique.

3 Sliding mode control

Traditionally, SMC is a non-linear strategy that forces the trajectories of a dynamic system to slide across a surface by applying a discontinuous control signal [33]. The SMC is known for its robustness, good dynamics, and simplicity [34]. In our case, we use two sliding surfaces which are defined as follows:

$$\begin{cases} S(I_{dr}) = I_{dr}^{*} - I_{dr} \\ S(I_{qr}) = I_{qr}^{*} - I_{qr} \end{cases} \quad (17)$$

During the sliding phase, in stable state, we have:

$$\begin{cases} \dot{S}(I_{dr}) = \dot{I}_{dr}^{*} - \dot{I}_{dr} \\ \dot{S}(I_{qr}) = \dot{I}_{qr}^{*} - \dot{I}_{qr} \end{cases} \quad (18)$$

Based on system (18) we can compute the equivalent control laws V_{rq}^{eq} and V_{rd}^{eq}.

$$\begin{cases} \dot{S}(I_{dr}) = -\dfrac{2L_S}{3MV_S}\dot{P}_s^{*} - (V_{qr} - R_r I_{qr} - s w_S \sigma I_{dr} - s\dfrac{MV_S}{Ls})\dfrac{1}{\sigma} \\ \dot{S}(I_{qr}) = -\dfrac{2L_S}{3MV_S}\dot{Q}_s^{*} + \dfrac{V_S}{w_S M} - (V_{rd} - R_r I_{dr} + s w_S \sigma I_{qr})\dfrac{1}{\sigma} \end{cases} \quad (19)$$

With:

$$V_{rq} = V_{rq}^{eq} + V_{rq}^{n} \quad (20)$$

$$V_{rd} = V_{rd}^{eq} + V_{rd}^{n} \quad (21)$$

During the sliding phase, in stable state, we have:

$$\begin{cases} \dot{S}(I_{dr}) = 0, \quad S(I_{dr}) = 0 \\ \dot{S}(I_{qr}) = 0, \quad S(I_{qr}) = 0 \end{cases} \quad (22)$$

Based on system (18) we can compute the equivalent control laws V_{rq}^{eq} and V_{rd}^{eq}.

$$\begin{cases} \dot{S}(I_{dr}) = -\dfrac{2L_S}{3MV_S}\dot{P}_s^{*} - (V_{rq}^{eq} - R_r I_{rq} - s w_S \sigma I_{rd} - s\dfrac{MV_S}{Ls})\dfrac{1}{\sigma} \\ \dot{S}(I_{qr}) = -\dfrac{2L_S}{3MV_S}\dot{Q}_s^{*} + \dfrac{V_S}{w_S M} - (V_{rd}^{eq} - R_r I_{rd} + s w_S \sigma I_{rq})\dfrac{1}{\sigma} \end{cases} \quad (23)$$

Using reached condition in Eq. (22), we can deduce:

$$\begin{cases} V_{rq}^{eq} = -\dfrac{2L_S}{3MV_S}\dot{P}_s^{*} + R_r I_{rq} + s w_S \sigma I_{rd} + s\dfrac{MV_S}{Ls} \\ V_{rd}^{eq} = -\dfrac{2L_S}{3MV_S}\dot{Q}_s^{*} + \dfrac{V_S \sigma}{w_S M} + R_r I_{rd} - s w_S \sigma I_{rq} \end{cases} \quad (24)$$

V_{dq}^{n} is the saturation function defined by:

$$V_{dq}^{n} = -K.sat(S_{dq}) \quad (25)$$

where, K determine the ability of overcoming the chattering

The SMC will exist only if the following condition is met:

$$S.\dot{S} < 0 \quad (26)$$

The SMC method gives better results than the classic methods such as DTC and direct FOC strategy. But there is a downside to this technique, which is oscillations. Several scientific works dealt with this problem in this technique, and among the designed solutions is the integration of this technique with intelligent techniques, such as neural networks and neuro-fuzzy algorithms. Several works have suggested second-order SMC controller to compensate for the traditional SMC control and to ameliorate the performances of the DFIG. On the other hand, the STSMC technique is a type of high-order SMC strategy. Among the advantages of this technique is that it is easy to use

and does not require the mathematical form of the studied system.

4 Proposed Nonlinear Controller

As it is known, the SMC strategy is among the most popular nonlinear techniques, the most widespread, and the most robust, and it depends on the variable structure system. However, its main drawback is the presence of oscillations, called chattering [23, 35]. The chattering problem is one of the biggest problems with the traditional SMC technique.

Several strategies have been designed in the literature to reduce the chattering phenomena. However, the high-order SMC strategy is considered one of the best alternatives to reduce chattering. The second-order version of high-order SMC algorithms, such as the twisting algorithm, the suboptimal algorithm, and the super-twisting algorithm (STA) aim to enforce in a finite time a sliding mode involving the sliding surface and its time derivative [20-23]. In this work, we have chosen the STA because of its advantages. Unlike the first two methods (twisting and suboptimal), the STA only uses the sliding surface and does not require its derivative. However, STA is only applicable for systems with relative degree one (control appears in the first derivative of the sliding surface).

The STA technique law is defined as follows [36]:

$$U = U_1(t) + U_2(t) \tag{27}$$

With:

$$\dot{U}_1 = \begin{cases} -U & if \quad |U| > U_M \\ -\alpha sign(S) & if \quad not \end{cases} \tag{28}$$

$$U_2 = \begin{cases} -\zeta |S_0|^{\delta} sign(S) & if \quad |U| > S_0 \\ -\zeta |S|^{\delta} sign(S) & if \quad not \end{cases} \tag{29}$$

where, S is the sliding surface.

To ensure system stability, α, ζ and δ must satisfy the following conditions:

$$\begin{cases} \alpha > \dfrac{C_0}{K_m} & 0 < \delta < 0.5 \\ \zeta^2 > \dfrac{4C_0K_M(\alpha + C_0)}{K_m^2 K_m(\alpha + C_0)} & if \quad \delta = 0.5 \end{cases} \tag{30}$$

where S_0, C_0, K_m and K_M are positive constants.

If $S_0 = \infty$, a simplified version of the STSMC algorithm will be given by:

$$\begin{cases} U = -\zeta |S|^{\delta} sign(S) + U_1 \\ \dot{U}_1 = -\alpha sign(S) \end{cases} \tag{31}$$

By replacing the sign function with a smooth function, the chattering problem can be decreased even more.

$$smooth(\mathrm{t}) = \frac{t}{|t| + \mu} \tag{32}$$

where, μ is a positive coefficient.

The stability condition is given by:

$$\dot{S} \times S < 0 \tag{33}$$

Eqs. (27) to (31) represent the classical STSMC controller and Fig. 3 shows the structure of the traditional STSMC method. On the other hand, to calculate the values for K1 and K2 of the traditional STSMC controller, we used the PSO algorithm. Using the PSO algorithm allows for less chattering phenomenon and improves the characteristics of the STSMC controller.

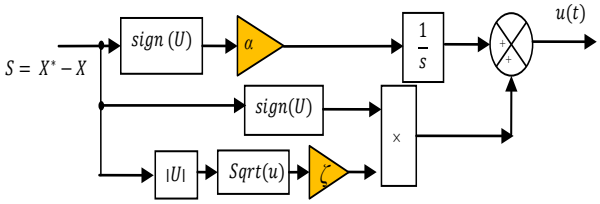

Fig. 3 Structure of the traditional STSMC controller.

In this section, a novel nonlinear controller was designed to minimize the undulations in the flux, voltage, active power, current, torque, and reactive power of the DFIG-based wind turbine. This new nonlinear controller is based on the combination of STSMC technique and PSO algorithm, to obtain a more robust nonlinear controller. Fig. 4 shows the structure of the designed PSO-STSMC controller.

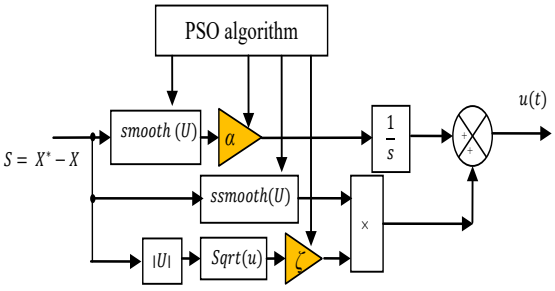

Fig. 4 Structure of the proposed PSO-STSMC controller.

Particle swarm optimization is a heuristic search strategy that is proposed by Kennedy and Eberhart in the mid-1990s [37]. It is based on the simulation of the social behavior and movement of individual

members in a bird flock or fish school searching for food sources. It works with a population called a swarm, and each individual is called a particle. This algorithm was used in many applications such as electronics, power, and control. In [38], a backstepping control scheme based on the PSO algorithm has been proposed to control the DFIG. This strategy provides advantages such as reduced power error, robustness against noise, and robustness against change in the DFIG parameters. In [39], a FOC technique based on the PSO algorithm has been designed to minimize the voltage, flux, current, and torque undulations of the DFIG. However, the proposed intelligent FOC technique is more simple structure and robust technique. In [40], the permanent magnet synchronous machine was controlled by using the PSO algorithm. The simulation results show the performances of the designed control strategy compared to the traditional technique.

The PSO's operation is as follows. During each iteration, each particle moves in searching space, looking for promising regions according to its own experiences and that of its neighbors. A general sketch of the PSO algorithm procedure can be described as [41-44]:

a. Initialization of the population (positions X_i^0 and velocities v_i^0 of particles) and control parameters (w, $c1$ and $c2$).

b. Evaluation of the objective function of each solution.

c. Update the global best solution (G_{besti}^k) and personal best solution (P_{besti}^k).

d. Update the velocities vi^{k+1} and positions Xi^{k+1} of particles by using the following equations:

$$\begin{cases} v_i^{k+1} = wv_i^k + c_1 r_1 (Pbest_i^k - X_i^k) + c_2 r_2 (Gbest_i^k - X_i^k) \\ r_1, r_2 \in [0,1] \ \ are \ \ random \ \ numbers \\ X_i^{k+1} = X_i^k + v_i^{k+1} \end{cases} \tag{34}$$

e. Repeat b, c and d until a termination condition has been reached.

To get the best parameters of the five STSMC controllers, an optimization problem is formulated by using the Integral Absolute Error (IAE) formulas, which is the sum of the absolute errors between the actual values of the currents, powers, and speed, and their reference values respectively:

$$IAE = \int \left(\left|\Delta\Omega_m\right| + \left|\Delta I_{rd}\right| + \left|\Delta I_{rq}\right| + \left|\Delta P_s\right| + \left|\Delta Q_s\right| \right) dt \tag{35}$$

where, $\Delta I_{rq} = I_{rq}^* - I_{rq}$, $\Delta I_{rd} = I_{rd}^* - I_{rd}$, $\Delta P_s = P_s^* - P_s$, $\Delta Q_s = Q_s^* - Q_s$, and $\Delta\Omega_m = \Omega_m^* - \Omega_m$

This proposed nonlinear controller (PSO-STSMC) is used in this work for minimizing active power, current, flux, torque, and reactive power undulations in a DFIG-based WP system using the indirect FOC technique in which the inverter was controlled by the PWM technique.

5 Proposed Nonlinear Indirect FOC Strategy

In this section, a novel indirect FOC technique was designed based on the PSO-STSMC technique. The proposed structure to control the DFIG-based WP system has five STSMC controllers with several parameters to tune, which is a very difficult task. For this reason, the PSO technique is used to find the optimal parameters of all STSMC regulators at the same time. The proposed nonlinear indirect FOC strategy is shown in Fig. 5. From this figure, five PSO-STSMC controllers are used in the indirect FOC technique, and one proposed PSO-STSMC controller was used in the MPPT technique. However, the proposed nonlinear indirect FOC technique is more robust compared to the classical FOC, DPC strategy, and DTC method. On the other hand, the proposed strategy of MPPT is used in calculating the reference value of the active power, where the active power becomes closely related to the wind speed.

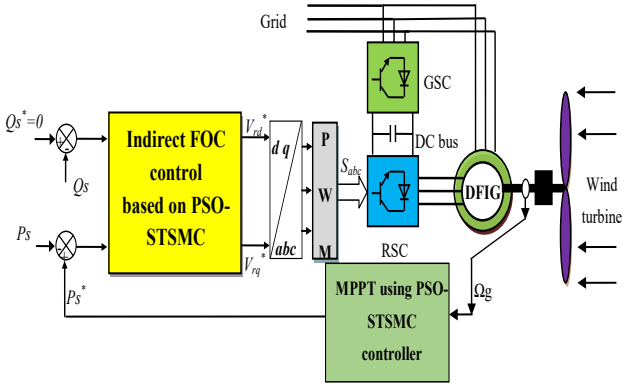

Fig. 5 Indirect FOC control using PSO-STSMC controller of the DFIG.

5.1 Wind Turbine Speed Control

The MPPT strategy aims to maximize energy extraction under all conditions. The tip speed ratio (TSR) technique is widely used, it is based on controlling the speed of the wind turbine to maximize the TSR [45, 46]. The structure of the designed turbine speed command is given in Fig. 6.

To design the proposed PSO-STSMC algorithm

of the turbine speed, the sliding surface is assumed to be equal to the mechanical speed error, as follows:

$$S(\Omega_m) = \Omega_m^* - \Omega_m \tag{36}$$

where, Ω_m and Ω^* are, respectively, the actual and the reference mechanical speed.

Using the definition of the proposed PSO-STSMC controller, the control law of the mechanical speed, which guarantees MPPT operation, is given by:

$$\begin{cases} T_{em}^* = -\zeta_1 \left|S(\Omega_m)\right|^{0.5} smooth(S(\Omega_m)) + T_1 \\ T_1 = -\int \alpha_1 smooth(S(\Omega_m))dt \end{cases} \tag{37}$$

where, T_{em}^* is the output of the proposed PSO-STSMC speed regulator, which represents the electromagnetic torque that the DFIG must generate.

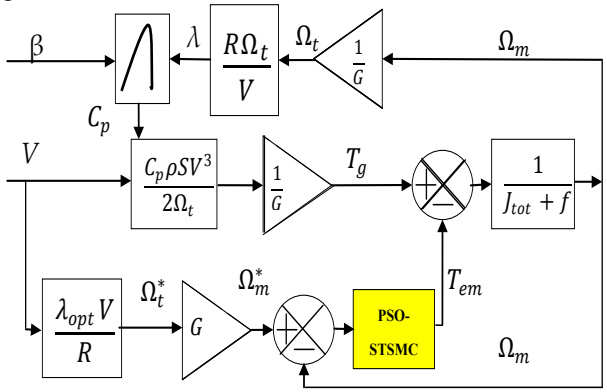

Fig. 6 Block diagram of proposed speed control.

5.2 Rotor Side Converter Control

The two most widely used methods of DFIG control are the stator FOC technique and the DPC strategy [11]. In this work, we used the indirect FOC technique to ensure indirect control of the powers injected into the grid. This technique is detailed in [47]. Through the study of several works, it was found that the FOC strategy is of two kinds, namely indirect and direct FOC techniques. In the direct technique, two PIs are used to regulate the active and reactive powers of the DFIG, while the indirect technique uses four PIs to regulate the stator active and reactive powers of the DFIG. So it can be said that the direct FOC strategy is more simple and can be accomplished easily compared to the indirect FOC technique. But the indirect FOC technique gives better results than the direct FOC technique in terms of current quality and effective power. Moreover, the indirect FOC technique gives a better value for the THD of the electric current compared to the direct FOC strategy. In this work, the indirect FOC technique is used based on the proposed PSO-STSMC technique to control and reduce the active power undulations of the DFIG. The principle of this technique is shown in Eq. (37) through (40) [48].

Equation (38) represents the direct and quadrature of the stator currents.

$$\begin{cases} I_{sd} = -\dfrac{M}{L_s} I_{rd} + \dfrac{\varphi}{L_s} \\ I_{sq} = -\dfrac{M}{L_s} I_{qr} \end{cases} \tag{38}$$

Equation (39) represents the direct and quadrature of the rotor voltages.

$$\begin{cases} V_{rq} = R_r I_{rq} + L_r \sigma w_r I_{rq} + s\dfrac{MV_s}{Ls} \\ V_{rd} = R_r I_{rd} - w_r L_r I_{rq} \end{cases} \tag{39}$$

Equations (40) and (41) represent the rotor fluxes and powers, respectively.

$$\begin{cases} \varphi_{rd} = L_r I_{rd} + \dfrac{MV_s}{w_s L_s} \\ \varphi_{rq} = L_r I_{rq} \end{cases} \tag{40}$$

$$\begin{cases} Q_S = \dfrac{V_S^2}{w_S L_S} - \dfrac{V_S M}{L_S} I_{rd} \\ P_S = -\dfrac{V_S M}{L_S} I_{rq} \end{cases} \tag{41}$$

From Eqs. (37) to (40), the internal structure of the traditional indirect FOC strategy can be given in Fig. 7. Through this figure, we note that this strategy controls the reactive and active power by controlling the quadrature and direct rotor voltages (V_{rd}* and V_{rq}*).

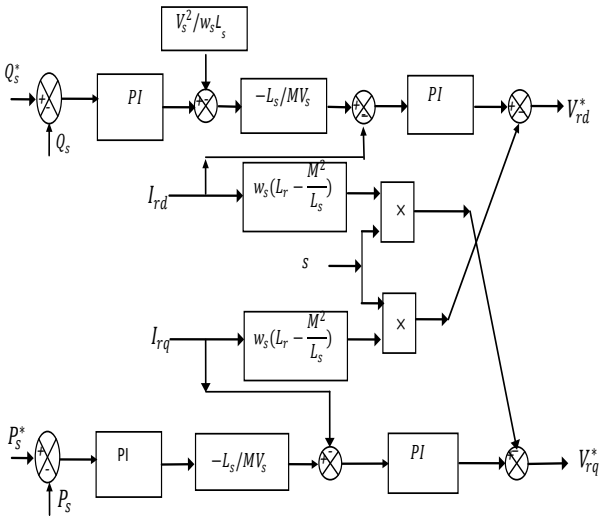

Fig. 7 Traditional indirect FOC technique.

Through this figure, we note that this strategy controls the reactive and active power by controlling the quadrature and direct rotor voltages (V_{rd}* and V_{rq}*). As shown in Fig. 7, two control loops are used in each axis, an outer loop to command the reactive/active power and an inner loop to control the *d-q* rotor currents I_{rq}/I_{rd} [14, 15]. The classical indirect FOC technique is a difficult strategy, not robust, and difficult to accomplish

compared to DTC and DPC techniques. This strategy gives more current, torque, flux, reactive power, and voltage ripples. This strategy has a long dynamic response compared to both DPC and DTC strategies. In addition, the indirect FOC strategy gives more THD value of voltage compared to the DTC technique.

To ameliorate the performance and efficacy of the traditional indirect FOC strategy, a new method for indirect FOC strategy is proposed in this section. This new indirect FOC strategy is based on the use of proposed PSO-STSMC strategies to replace the traditional PI controllers. In the proposed indirect FOC strategy based on the PSO-STSMC controller, two PSO-STSMC controllers were designed to control and regulate the direct rotor voltage and two PSO-STSMC controllers to control the quadrature rotor voltage. The proposed method is more robust compared to classical indirect FOC strategy, sliding mode control, DTC, and DPC strategies. Fig. 8 shows the designed indirect FOC strategy to regulate the reactive and active powers of the DFIG.

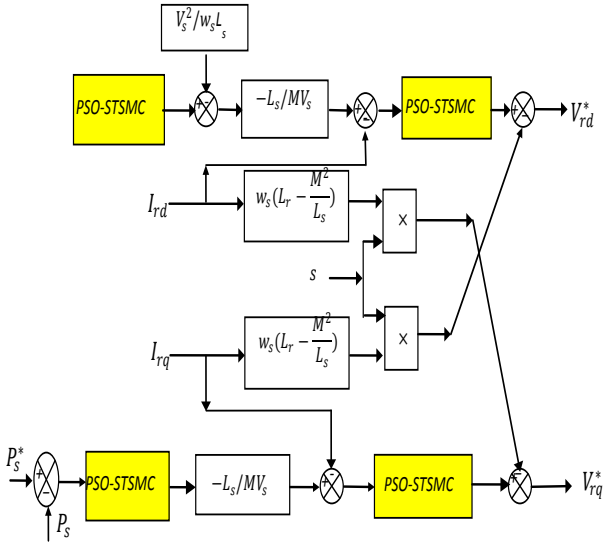

Fig. 8 Structure of the designed indirect FOC technique.

6 Simulations Results

To analyze the performance of the designed indirect FOC method based on the PSO-STSMC strategy, DFIG-based wind power is developed in MATLAB/Simulink and simulated for different wind speeds. In addition, the performance of the indirect FOC strategy based on the proposed PSO-STSMC controller is compared with that of the traditional SMC strategy. Tables 1 to 3 give the parameters of the DFIG, the grid side converter, and the wind turbine.

The profile of the wind speed used for the optimization process of the STSMC controllers is given in Fig. 9. In addition, the control parameters of the PSO algorithm are given in Table 4.

Table 1 The DFIG generator's parameters.

Parameter	Value
Stator peak phase voltage	380/690V
Magnetizing inductance	0.0025 H
Stator resistance	0.0026 Ω
Stator inductance	0.0026 H
Moment of inertia	127 Nm.s^2
Rotor resistance	0.0029 Ω
Number of pair of poles	2
Rotor inductance	0.0026 H

Table 2 A 2.4 MW wind turbines parameters.

Parameter	Value
Density of air ρ	1.225 Kg/m^3
Radius of rotor	47 m
Number of blade	3
Gear ratio	90

Table 3 The GSC'S parameters.

Parameter	Value
DC link voltage	1150 V
Filter inductance	0.0004 H
Filter resistance	0.0004 Ω
DC bus capacitance	0.08 F

Table 4 PSO method parameters.

Parameter	Value
Swarm size	50
Max iteration	100
c_1	0.1
c_2	1.2
w	0.8

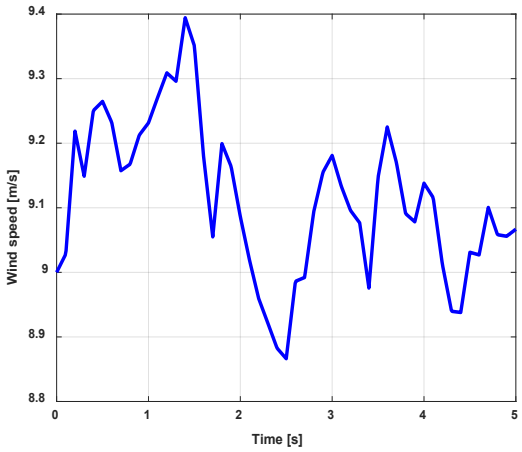

Fig. 9 Proposed wind profile.

The optimal parameters of the five STSMC regulators, obtained by the PSO algorithm, are given in Table 5.

Figure 10 shows that the turbine speed, obtained by the traditional SMC technique and proposed indirect FOC strategy based on designed PSO-STSMC controllers, closely follows the reference, which means that the DFIG injects into the grid the maximum power that can be extracted from the kinetic energy of the wind. However, the zoom on the speed, Fig. 11, shows that the speed obtained by the proposed indirect FOC strategy based on the designed PSO-STSMC strategy is closer to the reference than that obtained by the traditional SMC technique.

Table 5 Optimal parameters of STSMC controllers.

Sliding surface	Coefficient	Value
Turbine speed	ζ_1	29000000.5974
	μ_1	0.1491
	α_1	80515.4192
	μ_2	0.9164
Active power	ζ_2	12.1837
	μ_3	2550.0283
	α_2	50000.2548
	μ_4	100.4961
Quadrature axis rotor current	ζ_3	101.7892
	μ_5	10.5021
	α_3	2.2484
	μ_4	8.5822
Reactive power	ζ_4	115.2568
	μ_7	898.6486
	α_4	18560.3548
	μ_8	95.9845
Direct axis rotor current	ζ_5	55.6816
	μ_9	10.3215
	α_5	0.0235
	μ_{10}	95.6547

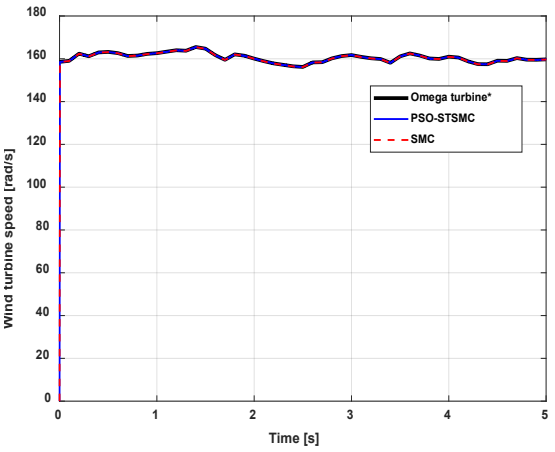

Fig. 10 Speed tracking performance.

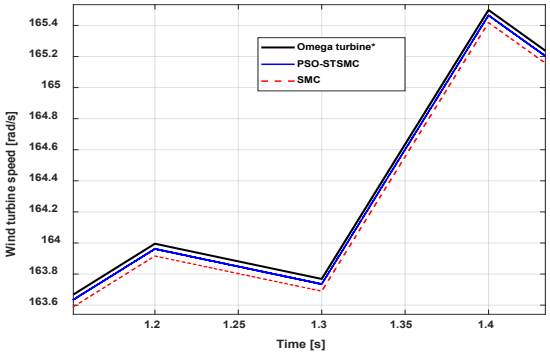

Fig. 11 Zoom on speed tracking performance.

Figure 12 and Fig. 13 show that powers track their references perfectly for the two control strategies (SMC technique and indirect FOC-PSO-STSMC strategy) and the performances are very close in terms of the overshoot and dynamic response.

Figure 14 and Fig. 15 represent the electric current produced by the SMC strategy and the proposed indirect FOC-PSO-STSMC strategy, respectively. Through these two figures, we can say that the shape of the current is sinusoidal and it is related to the active power as well as to the studied system.

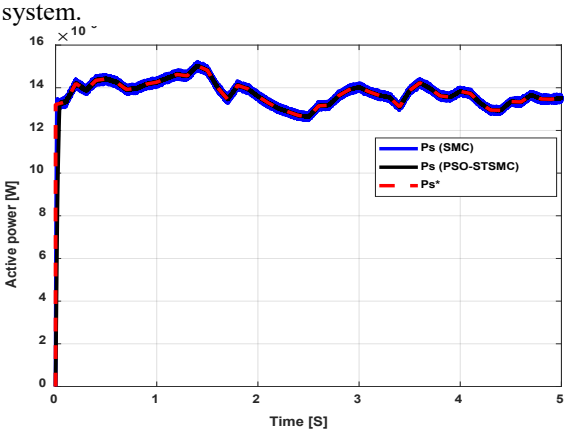

Fig. 12 The active stator power.

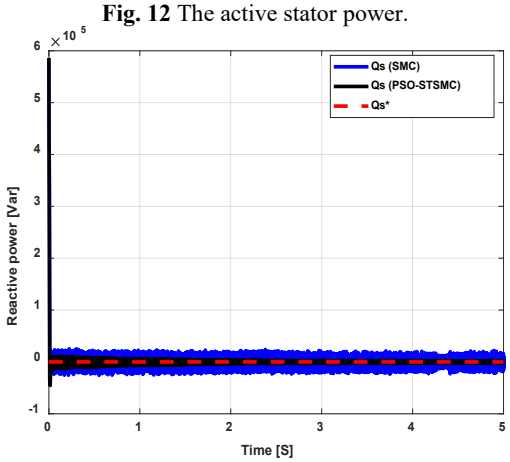

Fig. 13 The reactive stator power.

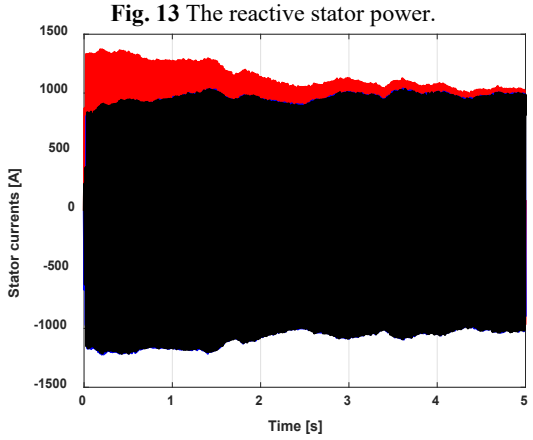

Fig. 14 Stator currents (SMC technique).

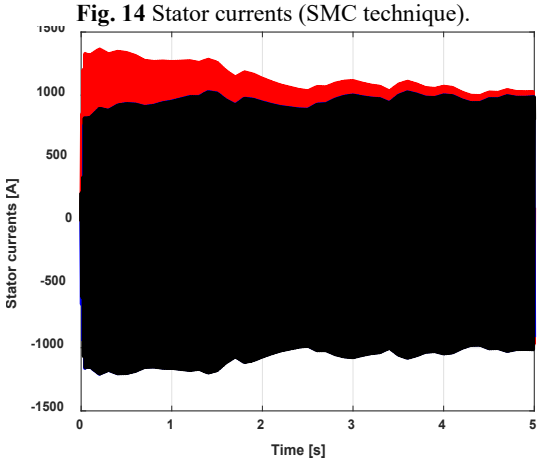

Fig. 15 Stator currents (Indirect FOC-PSO-STSMC).

The overshoot, SSE, and response time reduction values and percentages for each strategy are listed in Tables 6, 7, and 8, respectively. Through these tables, the proposed control provided good results in the case of overshoot, active power response time, and steady-state error. In Table 6, the proposed strategy reduced overshoot with very satisfactory percentages compared to the SMC control, where the percentages of reduction were 76.47% and 67.52% for each of, Active and reactive power, respectively.

In the case of SSE, the reduction ratios were 94.73% and 69.51% for both active and reactive power compared to the SMC control. Table 8 represents the response time for the active and reactive power, where the proposed control provided a better response time for the reactive power than the SMC control, where the reduction ratio was 37.50%. However, the proposed control presented an unsatisfactory time for the active power compared to the SMC control. So the response time of the active power is the negative of the proposed control.

Table 6 Overshoot value (First test).

Strategies	*Ps* (W)	*Qs* (VAR)
SMC	17000	44500
PSO-STSMC	4000	14450
Ratios	76.47%	67.52%

Table 7 The value of SSE (First test).

Strategies	*Ps* (W)	*Qs* (VAR)
SMC	19000	11640
PSO-STSMC	1000	3548
Ratios	94.73%	69.51%

Table 8 Time response value (First test).

Strategies	*Ps* (W)	*Qs* (VAR)
SMC	0.013 ms	0.012 ms
PSO-STSMC	0.05 ms	0.0075 ms
Ratios (%)	-74%	37.5%

Figure 16 and Fig. 17 show the zoom in the reactive power, active power, and stator current of both strategies, it is clear that there is a reduction in the power ripples obtained by the proposed indirect FOC-PSO-STSMC strategy. In addition, Fig. 18 and Fig. 19 show that the stator currents have good sinusoidal shapes without ripples, which implies clean energy without harmonics injected into the grid. In Table 9, the values and ripple reduction ratios for the active power, current, and reactive power for the control strategies used in this work are noted. Through this table, the proposed strategy reduced ripples in satisfactory proportions compared to the SMC control, where the reduction ratios were 90%, 48.21%, and 63.65% for current, active and reactive power, respectively. This result is expected since the proposed PSO-STSMC algorithm can considerably reduce the phenomenon of chattering.

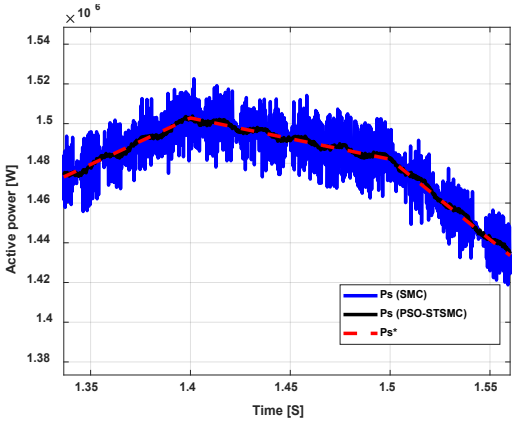

Fig. 16 Active power (Zoom).

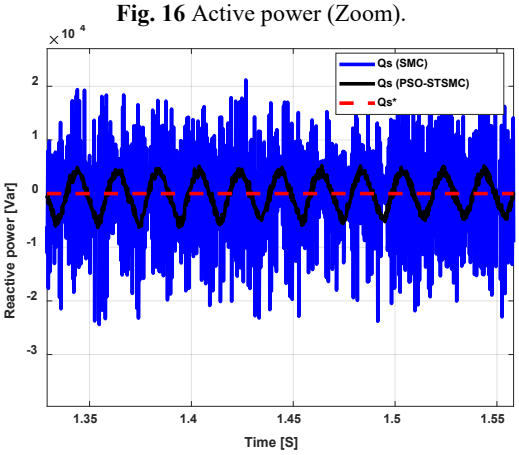

Fig. 17 Reactive power (Zoom).

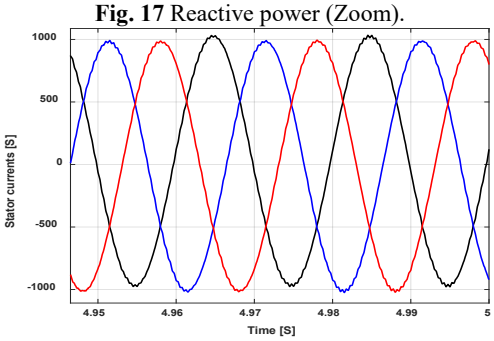

Fig. 18 Stator current of the SMC technique (Zoom).

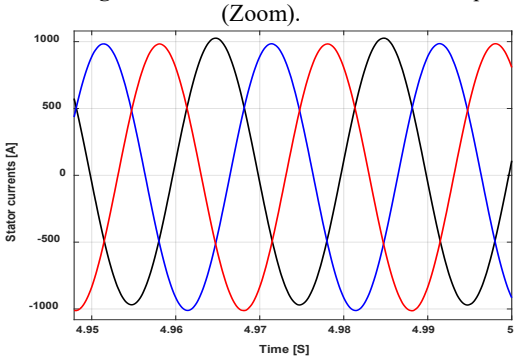

Fig. 19 Stator current of the indirect FOC-PSO-STSMC (Zoom).

Table 9 Ratios and power ripples (First test).

	Ia (A)	*Qs* (VAR)	*Ps* (W)
SMC	20	23620	27000
PSO-STSMC	2	3091	2000
Ratios	90%	86.91%	92.59%

Figure 20 shows the evolution of the DC link voltage. In this command loop, a simple PI controller is used. However, the performance is acceptable, and the voltage follows its reference of 1150 V.

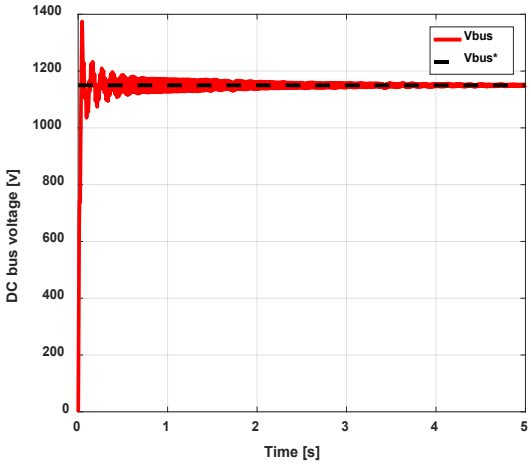

Fig. 20 The DC link voltage.

The THD value of the output current is shown in Figs. 21 and 22 for the two proposed control methods. From the two figures, it can be said that the designed indirect FOC-PSO-STSMC technique gave a lower value for THD of current compared to the SMC technique. The proposed indirect FOC-PSO-STSMC method reduced the value of THD of current by about 96.81% compared to the conventional SMC method.

6.1 Second Test

This test aims to ascertain the robustness of the designed technique and to know which strategy is not greatly affected by changing the DFIG parameters. In this test, R_r, R_s, L_s, L_r and M are all changed. In this test the value of the R_s and R_r are multiplied by 2 and L_m, L_r and L_s are multiplied by 0.5. The results obtained from this test are shown in Figs. 23 to 32. In this test, the measured active power and measured reactive power follow the reference values well for each of the two proposed control techniques, and this is seen in Figs. 23 and 24. However, the value of the active power is a value related to the wind speed, and this is because the reference value of the active power is obtained from the proposed MPPT technique based on PSO-STSMC strategy.

In this test, the reference value of the reactive power is made to zero. Figs. 25 and 26 represent the stator current produced by the generator using the SMC technique and the proposed indirect FOC-PSO-STSMC strategy, respectively. Through these two figures, it can be said that the current is related to the reference value of the active stator power, and it is a variable value. Where we find that the current follows the change in the reference active stator power.

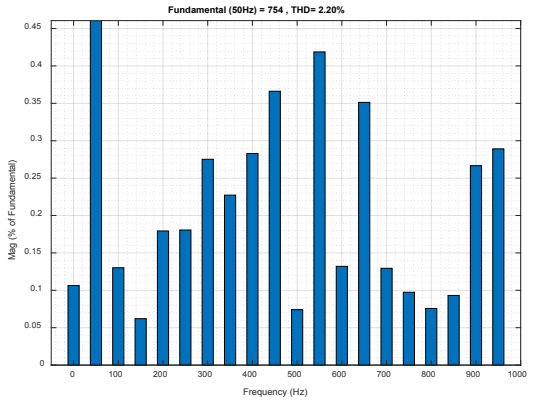

Fig. 21 THD value of current (SMC technique).

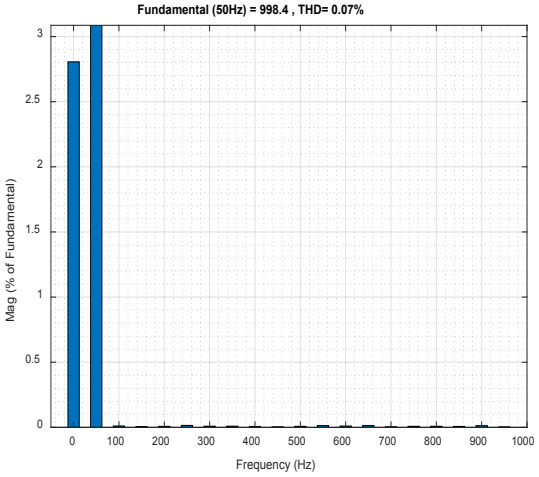

Fig. 22 THD value of currents (Indirect FOC-PSO-STSMC technique).

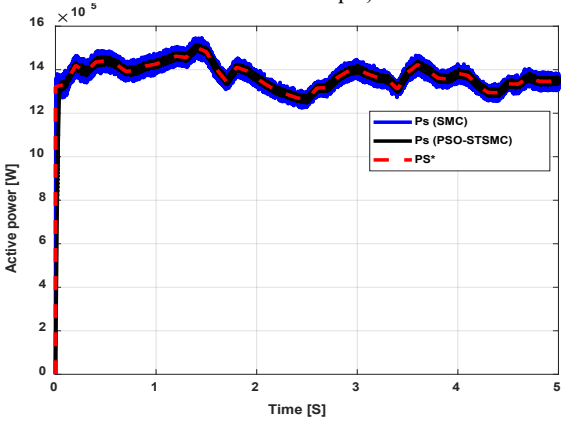

Fig. 23 Active power.

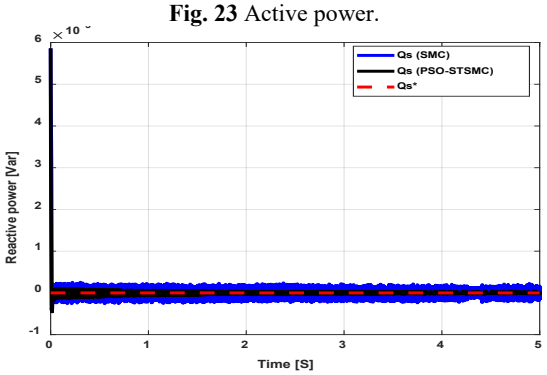

Fig. 24 Reactive power.

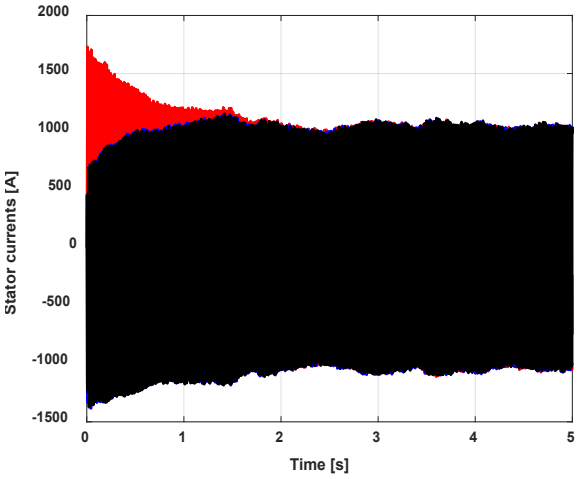

Fig. 25 Stator currents (SMC strategy).

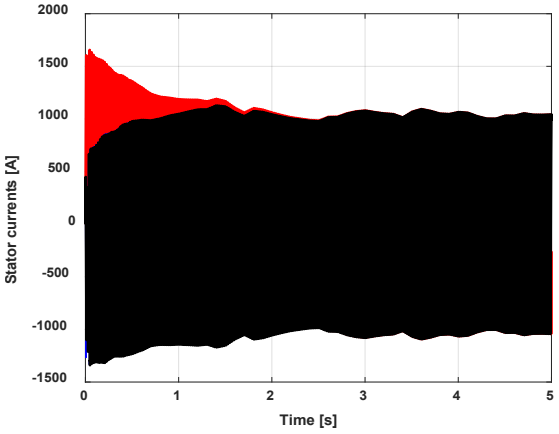

Fig. 26 Stator currents (Indirect FOC-PSO-STSMC strategy).

The electric current produced by the generator using traditional SMC technique and the proposed indirect FOC-PSO-STSMC strategy is shown in Figs. 25 and 26, respectively. Starting from the two figures, the stator current has a variable value for the two proposed control methods, and it is related to the reference value of the active power and the studied system as a whole.

The proposed indirect FOC-PSO-STSMC strategy reduced the current, active and reactive power undulations compared to classical SMC strategy (see Figs. 27-30). On the other hand, the values and ratios of ripple reduction for active power, current, and reactive power are shown in Table 10. Through this table, the proposed strategy reduced ripples in satisfactory proportions compared to the SMC control, where the reduction ratios were 48.07%, 48.21%, and 63.65% for current, active and reactive power, respectively.

Figures 31 and 32 show the THD value of stator current of both methods. From these figures, the proposed indirect FOC-PSO-STSMC strategy minimizes the THD value of stator current compared to classical SMC strategy and the reduction rate is about 62.72%.

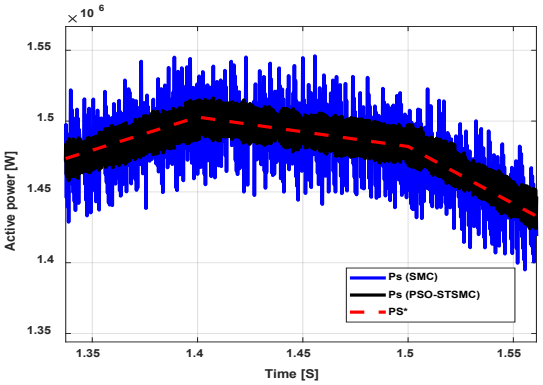

Fig. 27 Active power (Zoom).

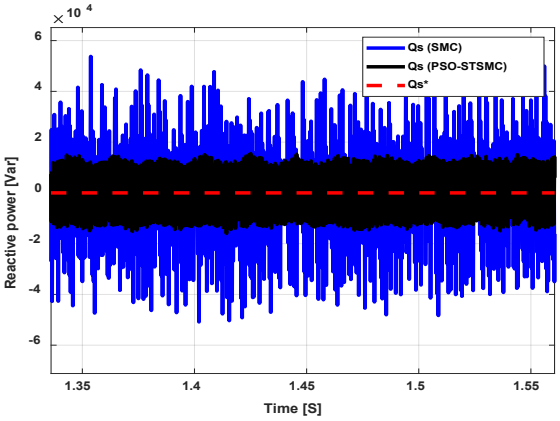

Fig. 28 Reactive power (Zoom).

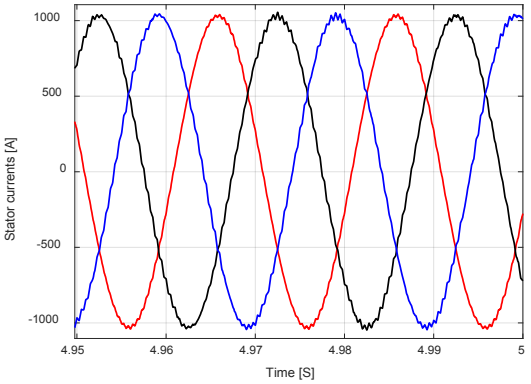

Fig. 29 Current of the SMC strategy (Zoom).

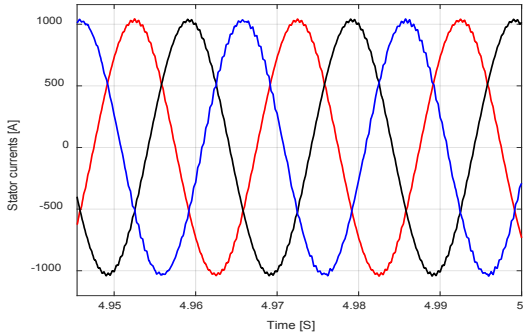

Fig. 30 Current of the indirect FOC-PSO-STSMC technique (Zoom).

Table 10 Ratios and ripple value (Second test).

	Ia (A)	*Qs* (VAR)	*Ps* (W)
SMC	52	64940	56000
PSO-STSMC	27	23600	29000
Ratios (%)	48.07	63.65	48.21

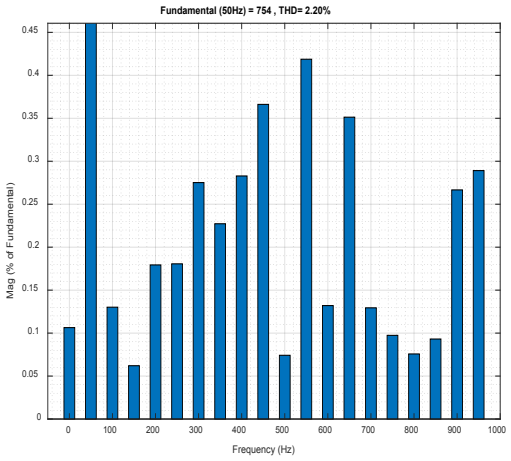

Fig. 31 THD value of the stator current (SMC).

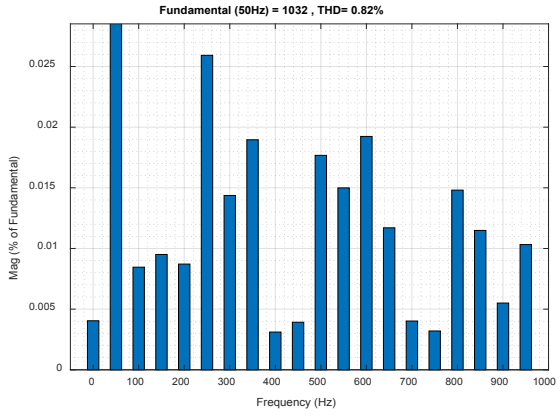

Fig. 32 THD value of the stator current (Indirect FOC-PSO-STSMC technique).

Tables 11-13 represent the overshoot, steady-state error, and response time reduction values and percentages for the proposed controls. From Tables 11, 12, and 13, the proposed control overshoot, active power response time, and steady-state error values are reduced. In Table 11, the overshoot reduction ratios for active and reactive power were 94.87% and 2.20%, respectively. The reduction ratios were 31.11% and 59.89% for active and reactive power, respectively, in the case of SSE (Table 12). Table 13 represents the values and reduction percentages of the response time for the active and reactive power, where the proposed control provided a better response time for the reactive power than the SMC control, where the reduction ratio was 37.50% (Table 13). However, the traditional control presented a response time to the active power compared to the proposed control.

Table 11 Overshoot value (**Second** test)

Strategies	Ps (W)	Qs (VAR)
SMC	39000	12680
PSO-STSMC	2000	12400
Ratios	94.87%	2.20%

Table 12 The value of SSE value (Second test)

Strategies	*Ps* (W)	*Qs* (VAR)
SMC	45000	31170
PSO-STSMC	31000	12500
Ratios	31.11%	59.89%

Table 13 Time response (Second **test**)

Strategies	*Ps* (W)	*Qs* (VAR)
SMC	0.006 ms	0.006 ms
PSO-STSMC	0.04 ms	0.003 ms
Ratios	-85%	50%

Table 14 represents a comparative study between the designed strategy and some published techniques in research work, where the comparison between the methods was made according to the obtained THD of current value. Through this table, we note that the designed indirect FOC strategy based on PSO-STSMC algorithms gave a much lower percentages of the THD of stator current than some of the published control strategies. So, it can be said that the proposed indirect FOC technique based on PSO-STSMC algorithms in this paper gives a sinusoidal current that has good performances in terms of ondulations and percentages of the THD of voltage compared to the rest of the published control strategies, and this is what makes the life of the devices longer and minimizes the cost of maintenance.

7 Conclusion

This paper presents the application of the designed PSO-STSMC controller to improve the characteristics of the indirect FOC technique and regulate the powers of the DFIG. The designed PSO-STSMC algorithm reduces the chattering phenomenon which characterizes the classical SMC strategy and at the same time ensures good robustness. However, the proposed PSO-STSMC technique contains more parameters to be tuned, which is a big challenge if the system is complex and contains multiple PSO-STSMC algorithms. For this reason, the PSO technique was used to obtain the optimal parameters of five STSMC regulators used in the MPPT strategy and reactive and active power control (indirect FOC strategy).

The simulation results confirm the good performance of the designed indirect FOC strategy based on PSO-STSMC algorithms in terms of dynamic response and reduction of current, active and reactive power oscillations. On the other hand, the proposed strategy reduced the value of THD by about 96.81% and 62.72% in the two proposed tests compared to the classical method (SMC).

So, the results obtained from this work can be summarized in the following points:

- A novel robust nonlinear controller based on the PSO technique was presented.
- The designed new robust nonlinear controller based on the PSO technique minimizes the undulations of current, flux, torque, and active power.
- The proposed indirect FOC technique improves the performance of the DFIG compared to the sliding mode control scheme.

In the next article, to improve the quality of the current generated by the asynchronous generator, a new and more robust nonlinear method will be proposed and the obtained results will be compared with this work. These methods that you will integrate are the PSO algorithm, fractional calculus, PI controller, and super twisting algorithm.

Table 14. A comparative study between the designed strategy and some published techniques in terms of THD value.

Reference	Strategy	THD (%)
Ref. [49]	DPC strategy with STSMC algorithm	1.66
Ref. [50]	DTC strategy	12
	DTC strategy with Ant Colony optimization algorithm	7.19
Ref. [51]	classical DTC method	6.70
	Fuzzy DTC strategy	2.40
Ref. [52]	Fuzzy SMC strategy	1.15
Ref. [53]	Fractional-order sliding mode control	1.31
Ref. [54]	Integral SMC (ISMC) strategy	9.71
	Multi-resonant-based SMC technique	3.14
Ref. [48]	Traditional FOC strategy	3.7
Ref. [55]	Backstepping control	2.19
Ref. [56]	Classical DTC strategy	11.17
	Fuzzy DTC strategy	1.73
Ref. [57]	Conventional DTC strategy	8.75
	Multilevel DTC strategy	1.57
Ref. [58]	DTC method	2.57
Ref. [59]	SOSMC strategy	3.13
Ref. [60]	Traditional direct vector control	1.65
Ref.[61]	Virtual flux DPC strategy	4.19
	Traditional DPC	4.88
Designed strategy: indirect FOC-PSO-STSMC technique	First test	1.05
	Second test	1.41

Acronyms

MPPT	Maximum power point tracking
THD	Total harmonic distortion
PI	Proportional integral
SSC	Stator side converter
TOSMC	Third-order sliding mode controller
ISMC	Integral sliding mode controller
PSO	Particle swarm optimization
DTC	Direct torque control
SMC	Sliding mode control
PWM	Pulse width modulation
DPC	Direct power control
SOSMC	Second-order sliding mode control
NN	Neural network
FOC	Field oriented control
HOSMC	High-order sliding mode controller
NSMC	Neural sliding mode control
DRWP	Dual-rotor wind power
SVM	Space vector modulation
IP	Integral-proportional
STSMC	Super twisting sliding mode controller
DFIG	Doubly-fed induction generator
MRSMC	Multi-resonant-based sliding mode controller
RSC	Rotor side converter

Nomenclature and symbols

ϕ_r, ϕ_r*	Actual and reference rotor flux
V_s, I_s	Vectors of the stator voltage and current
$Vr_{a,b,c}$, $Ir_{a,b,c}$	Rotor voltage and current in *abc* frame
$V_{\alpha,\beta}$, $I_{\alpha,\beta}$	Voltage and current in $\alpha\beta$ frame
T_e, T_e*	Actual and reference torques
ω_n, ω_r	Nominal and rotor speeds
R_s, R_r	Stator and rotor resistances
$\phi_{\alpha s}$, $\phi_{\beta s}$	Stator flux components in αβ frame
θr	Rotor flux angle
Ki, *Kp*	Integral and proportional gains
Lr,*Ls*, *M*	Rotor, stator and mutual inductances
P	Generator pole pairs
Wb	Weber (unit)
Hz	Hertz (unit)
Mw	Migawatt (unit)
mH	Millihenry (unit)
N.m	Newton-meter (unit)

Intellectual Property

The authors confirm that they have given due consideration to the protection of intellectual property associated with this work and that there are no impediments to publication, including the timing to publication, with respect to intellectual property.

Funding

This work is supported by the Ministry of Higher Education and Scientific Research of Algeria, as part of research project (PRFU N°, A01L07UN240120200002).

Credit Authorship Contribution Statement

H. Gasmi: Validation, software, methodology, resources, project administration, writing—original draft preparation. **M. Sofiane:** investigation, data curation. **H. Benbouhenni:** Validation, methodology, investigation, resources, project administration, writing—original draft preparation, supervision, Visualization, Formal analysis, Funding acquisition, writing—review and editing, writing—review and editing. **N. Bizon:** software, investigation, data curation, supervision, Visualization

Declaration of Competing Interest

The authors hereby confirm that the submitted manuscript is an original work and has not been published so far, is not under consideration for publication by any other journal and will not be submitted to any other journal until the decision

will be made by this journal. All authors have approved the manuscript and agree with its submission to "Iranian Journal of Electrical and Electronic Engineering".

References

[1] S. Zhou, F. Rong, X. Ning, "Optimization control strategy for large doubly-fed induction generator wind farm based on grouped wind turbine," *Energies*, Vol. 14, 4848, 2021.

[2] A. M. Eltamaly, M. Al-Saud, K. Sayed, A. G. Abo-Khalil, "Sensorless active and reactive control for DFIG wind turbines using opposition-based learning technique," *Sustainability*, Vol. 12, 3583, 2020.

[3] F. Amrane, A. Chaiba B. E. Babes S. Mekhilef, "Design and implementation of high performance field oriented control for grid-connected doubly fed induction generator via hysteresis rotor current controller," *Revue Roumaine Des Sciences Techniques*, Vol. 61, No. 4, pp. 319-324, 2016.

[4] E. Najib, D. Aziz, E. Abdelaziz, T. Mohammed, E. Youness, M. Khalid, B. Badre, "Direct torque control of doubly fed induction motor using three-level NPC inverter," *Protection and Control of Modern Power Systems*, Vol. 17, No. 4, pp. 1-9, 2019.

[5] M. Mazen Alhato, S. Bouallègue, H. Rezk, "Modeling and performance improvement of direct power control of doubly-fed induction generator-based wind turbine through second-order sliding mode control approach," *Mathematics*, Vol. 8, 2012, 2020.

[6] R. Prasad and N. P. Padhy, "Synergistic Frequency Regulation Control Mechanism for DFIG Wind Turbines With Optimal Pitch Dynamics," *IEEE Transactions on Power Systems*, Vol. 35, No. 4, pp. 3181-3191, 2020.

[7] L. Pan, Z. Zhu, Y. Xiong, J. Shao, "Integral Sliding Mode Control for Maximum Power Point Tracking in DFIG Based Floating Offshore Wind Turbine and Power to Gas," *Processes*, Vol. 9, 1016, 2021.

[8] Y. Djeriri, "Lyapunov-Based Robust Power Controllers for a Doubly Fed Induction Generator," *Iranian Journal of Electrical and Electronic Engineering*, Vol. 16, No. 4, pp. 551-558, 2020.

[9] H. Benbouhenni, N. Bizon, "Terminal synergetic control for direct active and reactive powers in asynchronous generator-based dual-rotor wind power systems," *Electronics*, Vol. 10, 1880, 2021.

[10] M. M. Alhato, M.N. Ibrahim, H. Rezk, S. Bouallègue, "An Enhanced DC-Link Voltage Response for Wind-Driven Doubly Fed Induction Generator Using Adaptive Fuzzy Extended State Observer and Sliding Mode Control," *Mathematics*, Vol. 9, 963, 2021.

[11] L. Shang, J. Hu, "Sliding-Mode-Based Direct Power Control of Grid-Connected Wind-Turbine-Driven Doubly Fed Induction Generators under Unbalanced Grid Voltage Conditions," *IEEE Transactions on Energy Conversion,* Vol. 27, No. 2, pp. 362-373, 2012.

[12] B. Habib, "Sliding mode with neural network regulateur for DFIG using two-level NPWM strategy," *Iranian Journal of Electrical & Electronic Engineering*, Vol. 15, No. 3, pp. 411-419, 2019.

[13] B. Habib, "A comparative study between FSMC and FSOSMC strategy for a DFIG-based wind turbine system," Majlesi Journal of Mechatronic Systems, Vol. 8, No.2, 2019.

[14] M. Adel, Al. Ahmed, D. Mahdi, A. Aman, E. Hisham, "Integral sliding mode control for back-to-back converter of DFIG wind turbine system," *The Journal of Engineering*, Vol. 2020, No.10, pp. 834-842, 2020.

[15] Y. Liu, W. Zhijie, X. Linyun, W. Jie, J. Xiuchen, "DFIG wind turbine sliding mode control with exponential reaching law under variable wind speed," *International Journal of Electrical Power & Energy Systems*, Vol. 96, pp. 253-260, 2018.

[16] A. Saghafinia, H.W. Ping, M.N. Uddin, K.S. Gaeid, "Adaptive Fuzzy Sliding-Mode Control Into Chattering-Free IM Drive," *IEEE Transactions on Industry Applications*, Vol. 51, No.1, pp. 692-701, 2015.

[17] N. Bounar, S. Labdai, A. Boulkroune, "PSO–GSA based fuzzy sliding mode controller for DFIG-based wind turbine," *ISA Transactions*, 2019.

[18] T. Orlowska-Kowalska, M. Kaminski, K. Szabat, "Implementation of a Sliding-Mode Controller with an Integral Function and Fuzzy Gain Value for the Electrical Drive with an Elastic Joint," *IEEE Transactions on Industrial Electronics*, Vol. 57, No. 4, pp. 1309-1317, 2010.

[19] I. Sami, S. Ullah, Z. Ali, N. Ullah, J.S. Ro, "A Super Twisting Fractional Order Terminal Sliding Mode Control for DFIG-Based Wind Energy Conversion System," *Energies*, Vol. 13, No.9, pp. 1-20, 2020.

[20] F.Z. Tria, K. Srairi, M.T. Benchouia, M. E. H. Benbouzid, "An integral sliding mode controller with super-twisting algorithm for

direct power control of wind generator based on a doubly fed induction generator," *International Journal of System Assurance Engineering and Management*, Vol. 7, No. 4, pp. 762-769, 2017.

[21] R. Sadeghi, S.M. Madani, M. Ataei, M.R. Agha Kashkooli, S. Ademi, "Super-Twisting Sliding Mode Direct Power Control of a Brushless Doubly Fed Induction Generator," *IEEE Transactions on Industrial Electronics*, Vol. 65, No. 11, pp. 9147-915, 2018.

[22] L. Djilali, A. Badillo-Olvera, Y. Yuliana Rios, H. López-Beltrán and L. Saihi, "Neural High Order Sliding Mode Control for Doubly Fed Induction Generator based Wind Turbines," *IEEE Latin America Transactions*, Vol. 20, No. 2, pp. 223-232, Feb. 2022.

[23] B. Habib, "Intelligent super twisting high order sliding mode controllers of dual-rotor wind power systems with a direct attack based on doubly fed induction generators," *Journal of Electrical Engineering, Electronics, Control and Computer Science-JEEECCS*, Vol. 7, No. 26, pp. 1-8, 2021.

[24] B. Habib, N. Bizon, "Improved rotor flux and torque control based on the third-order sliding mode scheme applied to the asynchronous generator for the single-rotor wind turbine," *Mathematics*, Vol. 9, No.18, 2297, 2021.

[25] B. Habib, "Amelioration effectiveness of torque and rotor flux control applied to the asynchronous generator (AG) for dual-rotor wind turbine using neural third-order sliding mode approaches," *International Journal of Engineering, Transactions C:Aspects*, Vol. 35, No.3, pp. 517-530, 2022.

[26] I. Yaichi, A. Semmah, P. Wira, Y. Djeriri, "Super-twisting sliding mode control of a doubly-fed induction generator based on the SVM strategy," *Periodica Polytechnica Electrical Engineering and Computer Science*, Vol. 63, No. 3, pp.178-190, 2019.

[27] J. Listwan, "Application of super-twisting sliding mode controllers in direct field-oriented control system of six-phase induction motor: experimental studies," *Power Electronics and Drives*, Vol. 3, No.1, pp. 23-34, 2018.

[28] B. Habib, Z. Boudjema, A. Belaidi, "Direct power control with NSTSM algorithm for DFIG using SVPWM technique*," Iranian Journal of Electrical & Electronic Engineering*, Vol. 17, No.1, pp. 1-11, 2021.

[29] B. Farid, B. Tarek, B. Sebti, "Fuzzy super twisting algorithm dual direct torque control of doubly fed induction machine," *International Journal of Electrical and Computer Engineering*, Vol. 11, No. 5, 2021.

[30] B. Habib, Z. Boudjema, A. Belaidi, "DPC based on ANFIS super-twisting sliding mode algorithm of a doubly-fed induction generator for wind energy system," *Journal Européen des Systèmes Automatisés*, Vol. 53, No.1, pp. 69-80, 2020.

[31] P. Cheng, C. Wu, F. Ning, J. He, "Voltage Modulated DPC Strategy of DFIG Using Extended Power Theory under Unbalanced Grid Voltage Conditions," *Energies*, Vol. 13, 6077, 2020.

[32] G. Brando, A. Dannier, I. Spina, "Performance Analysis of a Full Order Sensorless Control Adaptive Observer for Doubly-Fed Induction Generator in Grid Connected Operation," *Energies*, Vol. 14, 1254, 2021.

[33] J. Hu, H. Nian, B. Hu, Y. He, Z. Q. Zhu, "Direct Active and Reactive Power Regulation of DFIG Using Sliding-Mode Control Approach," *IEEE Transactions on Energy Conversion*, Vol. 25, No.4, pp. 1028-1039, 2010.

[34] M. I. Martinez, G. Tapia, A. Susperregui, H. Camblong, "Sliding-Mode Control for DFIG Rotor- and Grid-Side Converters Under Unbalanced and Harmonically Distorted Grid Voltage," *IEEE Transactions on Energy Conversion*, Vol. 27, No.2, pp. 328-339, 2012.

[35] I. Yaichi, A. Semmah, P. Wira, Y. Djeriri, "Super-twisting Sliding Mode Control of a Doubly-fed Induction Generator Based on the SVM Strategy," *Periodica Polytechnica Electrical Engineering and Computer Science*, 2019.

[36] M. Nasiri, S. Mobayen, Q.M. Zhu, "Super-twisting sliding mode control for gear less PMSG-based wind turbine," *Complexity*, Vol. 2019, 2019.

[37] W.-M. Lin, C.-M., Hong, C.-M. "Intelligent Approach to Maximum Power Point Tracking Control Strategy for Variable-Speed Wind Turbine Generation System," *Energy*, Vol. 35, pp. 2440-2447, 2010.

[38] H. Salmi, A. Badri, M. Zegrari, A. Sahel, A. Baghdad, "PSO-Backstepping controller of a grid connected DFIG based wind turbine," *International Journal of Electrical and Computer Engineering*, Vol. 10, No.1, pp. 856-867, 2020.

[39] C.-S. Wang, C.-W.S. Guo, D.-M. Tsay, J.-W. Perng, "PMSM Speed Control Based on Particle Swarm Optimization and Deep Deterministic Policy Gradient under Load Disturbance," *Machines*, Vol. 9, 343, 2021.

[40] Y. Li, B. Xiong, Y. Su, J. Tang, Z. Leng, "Particle Swarm Optimization-Based Power

and Temperature Control Scheme for Grid-Connected DFIG-Based Dish-Stirling Solar-Thermal System," *Energies*, Vol. 12, 1300, 2019.

[41] J. Kennedy, R. Eberhart, "Particle Swarm Optimization," *Proceedings of IEEE International Conference on Neural Networks*, pp. 1942-1948, 1995.

[42] R. Laina, F. Ez-Zahra Lamzouri, E.M. Boufounas, A. El Amrani, I. Boumhidi, "Intelligent control of a DFIG wind turbine using a PSO evolutionary algorithm," *Procedia Computer Science*, Vol. 127, pp. 471-480, 2018.

[43] D. Boudjehem, B. Boudjehem, "Improved heterogeneous particle swarm optimization," *Journal of Information and Optimization Sciences*, Vol. 38, No.3-4, pp. 481-499, 2017.

[44] S. Sai Rayala, N. Ashok Kumar, "Particle Swarm Optimization for robot target tracking application," *Materials Today: Proceedings*, 2020.

[45] V. Utkin, H. Lee, "Chattering problem in sliding mode control systems," *IFAC Proceedings*, Vol. 39, No.5, 2006.

[46] Y. Irfan, K. Y. Ersagun, "Improving Efficiency of the Tip Speed Ratio-MPPT Method for Wind Energy Systems by Using an Integral Sliding Mode Voltage Regulator," *Journal of Energy Resources Technology*, Vol. 140, No.5, 2018.

[47]F. Amrane, A. Chaiba, "A novel direct power control for grid-connected doubly fed induction generator based on hybrid artificial intelligent control with space vector modulation," Revue Roumaine Des Sciences Techniques, Vol. 61, No.3, pp. 263-268, 2016.

[48] K. Boulaam, A. Mekhilef, "Output power control of a variable wind energy conversion system," Rev. Sci. Techni.-Electrotechn. Et Energ., Vol. 62, No.2, pp. 197-202, 2017.

[49] I. Yaichi, A. Semmah, P. Wira, Y. Djeriri, "Super-twisting sliding mode control of a doubly-fed induction generator based on the SVM strategy," *Periodica Polytechnica Electrical Engineering and Computer Scienc*e, Vol.63, No.3, pp. 178-190, 2019.

[50] S. Mahfoud, A. Derouich, A. Iqbal, N. El Ouanjli, "Ant-Colony optimization-direct torque control for a doubly fed induction motor: An experimental validation," *Energy Reports*, Vol. 8, pp. 81-98, 2022.

[51] W. Ayrira, M. Ourahoua, B. El Hassounia, A. Haddib, "Direct torque control improvement of a variable speed DFIG based on a fuzzy inference system," *Mathematics and Computers in Simulation*, Vol. 167, pp. 308–324, 2020.

[52] Z. Boudjema, A. Meroufel, Y. Djerriri, E. Bounadja, "Fuzzy sliding mode control of a doubly fed induction generator for energy conversion," *Carpathian Journal of Electronic and Computer Engineering*, Vol. 6, No.2, pp.7-14, 2013.

[53] M. A. Beniss, H. El Moussaoui, T. Lamhamdi, H. El Markhi, "Improvement of power quality injected into the grid by using a FOSMC-DPC for doubly fed induction generator," *International Journal of intelligent Engineering & Systems*, Vol. 14, No. 2, pp. 556-567, 2021.

[54] Y. Quan, L. Hang, Y. He, Y. Zhang, "Multi-Resonant-Based Sliding Mode Control of DFIG-Based Wind System under Unbalanced and Harmonic Network Conditions," *Applied Sciences*, Vol. 9, 1124, 2019.

[55] Z. Zeghdi, L. Barazane, Y. Bekakra, A. Larbi, "Improved backstepping control of a DFIG based wind energy conversion system using ant lion optimizer algorithm," *Periodica Polytechnica Electrical Engineering and Computer Science*, Vol. 2021, pp.1-17, 2021.

[56] N. El Ouanjli, S. Motahhir, A. Derouich, A. El Ghzizal, A. Chebabhi, M. Taoussi, "Improved DTC strategy of doubly fed induction motor using fuzzy logic controller," *Energy Reports*, Vol.5, pp.271-279, 2019.

[57] N. El Ouanjli, D. Aziz, A. El Ghzizal, T. Mohammed, E. Youness, M. Khalid, B. Badre, "Direct torque control of doubly fed induction motor using three-level NPC inverter," *Protection and Control of Modern Power Systems*, Vol. 17, No.4, 1-9, 2019.

[58] Z. Boudjema, R. Taleb, Y. Djerriri, A. Yahdou, "A novel direct torque control using second order continuous sliding mode of a doubly fed induction generator for a wind energy conversion system," *Turkish Journal of Electrical Engineering & Computer Sciences*, Vol. 25, No. 2, pp. 965-975, 2017.

[59] A. Yahdou, B. Hemici, Z. Boudjema, "Second order sliding mode control of a dual-rotor wind turbine system by employing a matrix converter," *Journal of Electrical Engineering*, Vol.16, No. 3, pp. 1-11, 2016.

[60] H. Benbouhenni, N. Bizon, "Advanced direct vector control method for optimizing the operation of a double-powered induction generator-based dual-rotor wind turbine system," *Mathematics*, Vol.9, No.19, 2021.

[61] N. A. Yusoff, A. M. Razali, K. A. Karim, T. Sutikno, A. Jidin, "A Concept of virtual-flux direct power control of three-phase AC-

DC converter," *International Journal of Power Electronics and Drive System*, Vol. 8, No.4, pp. 1776-1784, 2017.

H. Gasmi was born in Skikda, Algeria. He received his M.S. degree in Electrical Engineering from Skikda University, Algeria in 2016, and PhD from Guelma University, Faculty of Technology, Algeria in 2023. His research interests include power electronics, electric machines, and renewable energy.

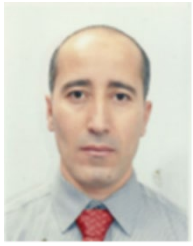

S. Mendaci was born in Jijel, Algeria. He received his B.S. degree in Electrical Engineering from Jijel University, Algeria in 2000; M.S. degree from BATNA University, Algeria in 2003; and PhD from Jijel University, Algeria in 2013. He is currently an Assistant Professor at the University of Guelma, Algeria. His research interests include design and control of electrical machines.

H. Benbouhenni was born in chlef, Algeria. He holds a degree in Engineering in Electronics from the National Polytechnic School Maurice Audin Oran (ENPO-MA), Algeria. In 2017, she obtained a Magister degree in Automatic and informatique industrial from the same school. He also holds a PhD in Electrical Engineering from the ENPO-MA. He is currently professor with the University of Nisantasi, Turkey. He is editor of seven books and more than 170 papers in scientific fields related to electrical engineering. His research activities include the application of robust control in the wind turbine power systems.

N. Bizon (IEEE M'06; SM'16), was born in Albesti de Muscel, Arges county, Romania, 1961. He received the B.S. degree in electronic engineering from the University "Polytechnic" of Bucharest, Romania, in 1986, and the PhD degree in Automatic Systems and Control from the same university, in 1996. From 1996 to 1989, he was in hardware design with the Dacia Renault SA, Romania. He is currently professor with the University of Pitesti, Romania. He received two awards from Romanian Academy, in 2013 and 2016. He is editor of ten books and more than 500 papers in scientific fields related to Energy. His current research interests include power electronic converters, fuel cell and electric vehicles, renewable energy, energy storage system, microgrids, and control and optimization of these systems.